IEEE Access
Multidisciplinary : Rapid Review : Open Access Journal

Received April 24, 2022, accepted May 10, 2022, date of publication May 16, 2022, date of current version May 23, 2022.

Digital Object Identifier 10.1109/ACCESS.2022.3175207

Bidirectional Power Control Strategy for Super Capacitor Energy Storage System Based on MMC DC-DC Converter

ZHICHAO ZHU[1], FEI XIAO[1], ZHAOJIE HUANG[1], JILONG LIU[1], PENG CHEN[2], AND QIANG REN[1]

[1]National Key Laboratory of Science and Technology on Vessel Integrated Power System, Naval University of Engineering, Wuhan 430000, China

[2]School of Electrical Engineering, Southeast University, Nanjing 211189, China

Corresponding author: Zhaojie Huang (18696422297@163.com)

This work was supported by the National Natural Science Foundation of China under Grant 51807200.

ABSTRACT In order to equip more high-energy pulse loads and improve power supply reliability, the vessel integrated power system (IPS) shows an increasing demand for high-voltage and large-capacity energy storage systems. Based on this background, this paper focuses on a super capacitor energy storage system based on a cascaded DC-DC converter composed of modular multilevel converter (MMC) and dual active bridges (DAB). The cascaded converter is called MMC-DAB for short. This paper analyzes the topology and modulation strategy of the system in detail. Taking into account the shortcomings of the traditional bidirectional power control strategy, this paper proposes a control strategy where the DAB module of each branch independently controls the voltage of the sub-module capacitor. The mathematical models of the traditional and the proposed control strategy are established. The stability of the two control strategies is analyzed and compared. Finally, a MW-level engineering prototype of the MMC-DAB energy storage system is designed and manufactured, and the effectiveness of the proposed control strategy was verified through experiments.

INDEX TERMS Vessel integrated power system, super capacitor energy storage system, bidirectional power control, sub-module capacitor voltage control.

I. INTRODUCTION

The vessel integrated power system has received extensive attention in the fields of ship propulsion, ship informatization, and DC power distribution. In the future, IPS will be one of the inevitable technical routes for renewable energy ships [1]–[3]. In recent years, with the increasing demand for higher ship power supply reliability, and equipment of pulsed loads and new high-energy weapons, energy storage systems have become an indispensable part of the second-generation IPS [4], [5]. Therefore, the energy storage converter connected to the IPS medium voltage DC (MVDC) grid needs to be characterized by high voltage and large capacity, voltage conversion, electrical isolation and bidirectional conversion.

In order to match the MVDC power grid, the converter can adopt series-parallel technology, among which the input series output parallel (ISOP) structure is the most commonly used structure, which can improve the voltage and current level of the converter [6]. In [7], a power electronic transformer consisted of H-bridges cascaded by DABs is proposed to improve the power level of the train traction system. In literature [8], [9], multiple standardized DC-DC converters are combined in series and parallel to improve the modularity, and enhance the voltage and current level of the converter. However, most of the above topologies adopt centrally series-connected capacitors, and feature poor fault redundancy capability, so they are not suitable for occasions with high requirements on power supply reliability and continuity.

MMC is widely used in high-voltage and large-power applications because of its modular structure and fault tolerance [10]. For high-voltage rail transit vehicles, the control strategies of super capacitor energy storage system based on MMC are studied in [11], [12]. These two papers realize the

The associate editor coordinating the review of this manuscript and approving it for publication was Sze Sing Lee.

balanced decoupling control of the power of super capacitors, and put forward the corresponding energy management strategies. In [13], the control strategy of modular multilevel energy storage system under two operating conditions of grid voltage symmetry and asymmetry is studied, which solves the problem of charge state balance of energy storage elements. In [14], a fault diagnosis method based on the combination of simple hardware detection circuit and Field Programmable Gate Array (FPGA) diagnosis algorithm for MMC super capacitor energy storage system is proposed, so as to improve the safety and reliability of the system. Although the energy storage system based on MMC can solve the problems of MVDC grid access and fault tolerance, it can't realize the electrical isolation between MVDC bus and low voltage DC (LVDC) bus, and has high requirements for the design of power control strategy.

To realize the electrical isolation and voltage conversion, isolated bidirectional DC-DC converter needs to be used between MVDC grid and LVDC grid. DAB is a bidirectional DC-DC converter with electrical isolation capability and modular symmetrical structure. It has attracted extensive attention in the fields of electric vehicles, DC microgrids and energy storage systems [15]–[17]. In [18], [19], a solid-state transformer is proposed, which adopts the cascaded structure of half-bridge sub-module and DAB as the branch topology and ISOP as the overall structure. This topology is suitable for MV distribution network, because it is conducive to the realization of modular design and fault tolerance. In [20], a three port DC-DC converter composed of MMC, DAB and duplicate chopper circuits for IPS is proposed, which realizes the flexible power control among the MVDC grid, LVDC grid and distributed energy storage units.

However, the above literatures study the application scenario of connecting resistive load on the LVDC bus of MMC-DAB. Their control strategy is that MMC controls the voltage of sub-module capacitors and DAB controls the voltage of the LVDC bus. If this strategy is extended to the application scenario with energy storage unit connected on the LVDC side, the DAB module usually controls the port current of the energy storage unit. To better control the port current of the energy storage unit, the filter inductor needs to be connected between the DAB converter and the energy storage unit. However, this will increase the volume and weight of the device, and the stability margin of DAB control system is small. Especially when discharging the super capacitor, the filter inductor and the filter capacitor at the later stage of DAB form an LC filter with large output impedance, which is easy to cause cascaded stability problems [21].

Based on the above analysis, to meet the application requirements of the vessel integrated power system, this paper studies the control strategy and stability of super capacitor energy storage system based on MMC-DAB. The main innovations of this paper are as follows: (1) the bidirectional power conversion of a super capacitor energy storage system based on MMC-DAB is studied and a control strategy based on independent control of sub-module capacitor voltage is proposed. (2) A 1MW engineering prototype of MMC-DAB energy storage system is designed and manufactured to validate the proposed control strategy.

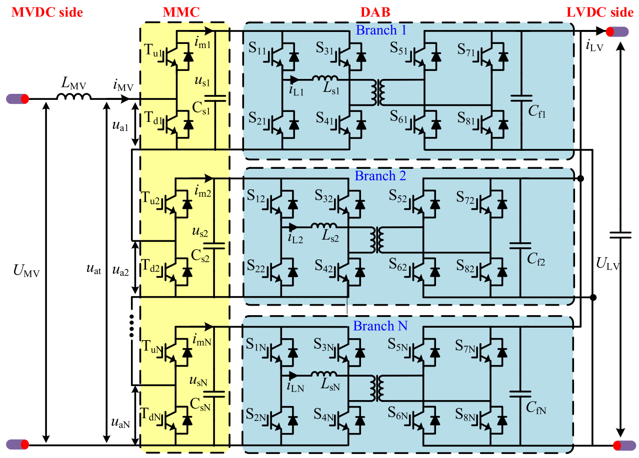

FIGURE 1. Topology of super capacitor energy storage system based on MMC-DAB.

The sections of this paper are organized as follows: In Section II, the topology and basic principle of the cascaded energy storage system based on MMC-DAB are introduced. In Section III, the traditional control strategy is analyzed, and the mathematical model of the traditional control strategy is established. Besides, the stability of the closed-loop control system of DAB is analyzed. In Section IV, the strategy based on independent control of sub-module capacitor voltage is proposed, and the stability of the proposed strategy is modeled and compared. In Section V, a 1MW engineering prototype is established and the above theory is verified by experiments. Conclusion is made in Section VI.

II. TOPOLOGY AND BASIC PRINCIPLE OF SUPER CAPACITOR ENERGY STORAGE SYSTEM BASED ON MMC-DAB

A. TOPOLOGY OF MMC-DAB

The topology of the super capacitor energy storage system based on the MMC-DAB, which is composed of N branches, is presented in Fig. 1. MMC structure with N half bridge sub-modules in series is adopted at the MVDC side to improve the power system capacity, voltage level and fault-tolerant operation ability. DAB is adopted at the LVDC side to provide electrical isolation. The super capacitor energy storage unit is connected to the LVDC bus to realize bidirectional power conversion with the MVDC bus.

MMC-DAB is characterized by bidirectional power conversion, high degree of modularity and fault tolerance, which can meet the needs of integration of high-voltage large-capacity energy storage unit and improvement power supply reliability. In Fig. 1, U_{MV} and i_{MV} are the voltage and current of the MVDC bus, respectively. U_{LV} and i_{LV} are the voltage and current of the LVDC bus, respectively. C_{si} and u_{si} are the capacitance and voltage of the i-th sub-module of MMC, respectively. L_{MV} is the inductance on the MVDC side. C_{fi} is the filter capacitor of each branch on the LVDC side. L_{si} and i_{Li} are the leakage inductance and leakage inductance current of the transformer of each branch.

B. PRINCIPLE OF MMC

MMC is composed by series-connected half bridge sub-modules. When the branch fails, it can quickly cut off the whole branch through bypassing the sub module to support the continuous operation of the energy storage system. To reduce the current ripple on the MVDC side, MMC adopts carrier phase-shift modulation. The driving pulse signals of the upper and lower switches of the same half bridge sub-modules are complementary. The phase-shift angle of the driving pulse signals of the corresponding switches of adjacent sub-modules is $2\pi/N$, and N is the number of sub-modules. Considering the relationship between the duty cycle of the upper switch and the carrier phase-shift angle, a switching cycle T_{m} is divided into N parts. Within each part, the total cascaded input voltage of the MMC u_{at} has only two levels, and the difference between the two voltage levels is $U_{\mathrm{s}i}$.

It is assumed that the capacitor voltage and the power of the sub-module of each branch of MMC is balanced, which means the duty cycle of each sub-module is consistent. According to KVL, the state equation of inductance on the MVDC side is listed as (1).

$$L_{\mathrm{MV}}\frac{di_{\mathrm{MV}}}{dt} = u_{\mathrm{MV}} - u_{\mathrm{at}} \tag{1}$$

When the converter is running in a steady state, the inductance on the MVDC side reaches the volt-second balance, which satisfies the following relationship.

$$U_{\mathrm{MV}} = ND_{\mathrm{m}}U_{\mathrm{s}i} \tag{2}$$

$$i_{\mathrm{m}i} = D_{\mathrm{m}}i_{\mathrm{MV}} \tag{3}$$

where D_{m} is the duty cycle of the upper switch of the half bridge sub-modules, and $i_{\mathrm{m}i}$ is current of the i-th sub-module of MMC.

Therefore, in the steady-state operation of the converter, the power of a single branch $P_{\mathrm{s}i}$ is expressed as:

$$P_{\mathrm{s}i} = U_{\mathrm{s}i}i_{\mathrm{m}i} = D_{\mathrm{m}}U_{\mathrm{s}i}i_{\mathrm{MV}} \tag{4}$$

According to (4), the branch power can be adjusted by adjusting the duty cycle and capacitor voltage $U_{\mathrm{s}i}$ of the sub-module.

C. PRINCIPLE OF DAB

As shown in Fig. 2, the topology of DAB is composed of two H-bridges and high-frequency transformers. In Fig. 2, u_{s} is the DAB high-voltage side port voltage. u_{LV} is the DAB low-voltage side port voltage. n_{T} is the transformation ratio of the high-frequency transformer. C_{f} is the low-voltage side filter capacitor. $C_{\mathrm{sc}i}$ and R_{esr} are the capacitance and resistance of the equivalent supercapacitor of each branch. When operating within the rated voltage range of the energy storage unit, through the implementation of voltage matching control, the DAB can match the sub-module voltage on the

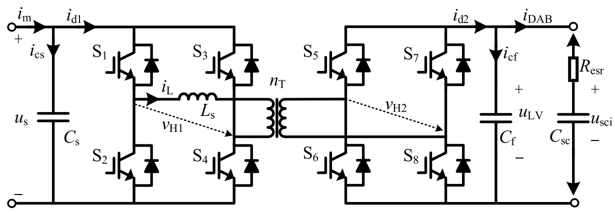

FIGURE 2. Topology structure of DAB module.

high-voltage side with the voltage of the energy storage unit on the LVDC side, which is conducive to optimizing the high-frequency circulation characteristics and current stress of the DAB, which improves the efficiency of the system. Therefore, the single-phase shift (SPS) modulation is used in this paper.

The dynamic equation of the equivalent circuit is deduced by Kirchhoff's law as follows.

$$v_{\mathrm{H1}} - n_{\mathrm{T}}v_{\mathrm{H2}} - L_{\mathrm{s}}\frac{di_{\mathrm{L}}(t)}{dt} = 0 \tag{5}$$

Integrating the inductance current of half switching cycle and considering the symmetry of leakage inductance current, the transmission power model of DAB can be obtained as

$$P_{\mathrm{DAB}} = \frac{1}{T_{\mathrm{d}}}\int_0^{T_{\mathrm{d}}} v_{\mathrm{H1}}(t)i_{\mathrm{L}}dt = \frac{U_{\mathrm{s}}U_{\mathrm{LV}}}{2L_{\mathrm{s}}f_{\mathrm{d}}}d_{\mathrm{d}}\left(1-d_{\mathrm{d}}\right) \tag{6}$$

where, U_{s} and U_{LV} are the amplitude of square waves v_{H1} and v_{H2} converted to the high voltage side, and d_{d} is the outer phase-shift ratio in half a switching cycle. f_{d} and T_{d} are the switching frequency and switching period of the DAB converter.

To establish the state average model of the DAB converter, according to (6), the DAB input average current i_{d1} and the converted output average current i_{d2} can be expressed as

$$\begin{aligned} i_{\mathrm{d1}} &= \frac{u_{\mathrm{LV}}}{2L_{\mathrm{s}}f_{\mathrm{d}}}d_{\mathrm{d}}\left(1-d_{\mathrm{d}}\right) \\ i_{\mathrm{d2}} &= \frac{u_{\mathrm{s}}}{2L_{\mathrm{s}}f_{\mathrm{d}}}d_{\mathrm{d}}\left(1-d_{\mathrm{d}}\right) \end{aligned} \tag{7}$$

To obtain the small-signal mathematical model of DAB, the small-signal perturbation method is used. Small-signal perturbation around the steady state values of the state variables are introduced such that, $u_{\mathrm{s}} = U_{\mathrm{s}} + \hat{u}_{\mathrm{s}}$, $u_{\mathrm{LV}} = U_{\mathrm{LV}} + \hat{u}_{\mathrm{LV}}$, $i_{\mathrm{d1}} = I_{\mathrm{d1}} + \hat{i}_{\mathrm{d1}}$, $i_{\mathrm{d2}} = I_{\mathrm{d2}} + \hat{i}_{\mathrm{d2}}$, $d_{\mathrm{d}} = D_{\mathrm{d}} + \hat{d}_{\mathrm{d}}$. Then, the final mathematical model can be simplified as (8).

$$\begin{aligned} \hat{i}_{\mathrm{d1}} &= \frac{D_{\mathrm{d}}(1-D_{\mathrm{d}})}{2L_{\mathrm{s}}f_{\mathrm{d}}}\hat{u}_{\mathrm{LV}} + \frac{U_{\mathrm{LV}}(1-2D_{\mathrm{d}})}{2L_{\mathrm{s}}f_{\mathrm{d}}}\hat{d}_{\mathrm{d}} \\ \hat{i}_{\mathrm{d2}} &= \frac{D_{\mathrm{d}}(1-D_{\mathrm{d}})}{2L_{\mathrm{s}}f_{\mathrm{d}}}\hat{u}_{\mathrm{s}} + \frac{U_{\mathrm{s}}(1-2D_{\mathrm{d}})}{2L_{\mathrm{s}}f_{\mathrm{d}}}\hat{d}_{\mathrm{d}} \end{aligned} \tag{8}$$

where, let

$$g_1 = \frac{D_{\mathrm{d}}(1-D_{\mathrm{d}})}{2L_{\mathrm{s}}f_{\mathrm{d}}},\ g_2 = \frac{U_{\mathrm{LV}}(1-2D_{\mathrm{d}})}{2L_{\mathrm{s}}f_{\mathrm{d}}},\ g_3 = \frac{U_{\mathrm{s}}(1-2D_{\mathrm{d}})}{2L_{\mathrm{s}}f_{\mathrm{d}}}$$

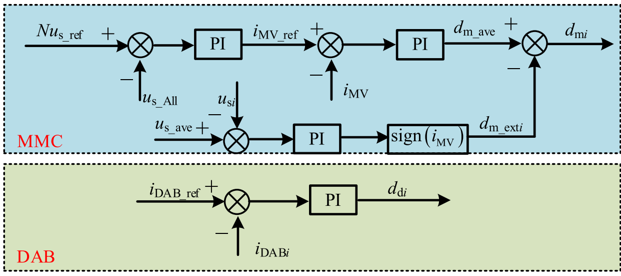

FIGURE 3. Block diagram of traditional control strategy of MMC-DAB.

III. TRADITIONAL CONTROL STRATEGY AND MODELING

As shown in Fig. 3, under the traditional control strategy, the control strategy of MMC is a dual closed-loop control with the sub-module capacitor voltage and the current of the MVDC bus as the control objectives, and the control strategy of DAB converters is a closed-loop control with the LVDC side current of each branch as the control objective. The reference value of the current of the MVDC bus is generated by the outer voltage loop of the controller of MMC, and the shared duty cycle d_{m_ave} of sub-modules is generated through the PI regulator of the inner loop. Considering the difference of branches, the compensation duty cycle d_{m_exti} is generated by the sub-module voltage balancing regulator to equalize the capacitance voltage of the sub-module.

In Fig. 3, Nu_{s_ref} and u_{s_All} are respectively the sum of the reference value and the actual value of the capacitance voltage of all sub-modules. u_{si} and u_{s_ave} are respectively the actual value and average value of the capacitance voltage of each sub-module. i_{MV_ref} and i_{MV} are the reference value and actual value of the current of the MVDC bus respectively.

When the DAB converter is connected with energy storage units such as super capacitor, the charging or discharging current is difficult to control. Therefore, a filter inductor needs to be set between the DAB and the super capacitor. At this time, the DAB adopts single-loop current control. Since the voltage at the high voltage side of DAB is controlled by MMC under the traditional control strategy, the capacitance voltage of sub-module can be equivalent to voltage source when analyzing the mathematical model of DAB.

As shown in Fig.4, from the small signal model of DAB under the traditional control strategy, the state equation of DAB is written as,

$$\begin{cases} C_f \dfrac{d\hat{u}_{LV}}{dt} = \hat{i}_{d2} - \hat{i}_{Lf} = g_3\hat{d}_d + g_1\hat{u}_s - \hat{i}_{Lf} \\ L_f \dfrac{d\hat{i}_{Lf}}{dt} = \hat{u}_{LV} - \hat{u}_{sc} - \hat{i}_{Lf}R_{esr} \end{cases} \tag{9}$$

The Laplace transformation is implemented on the state space equation, and the expression of the system transfer function matrix is obtained as,

$$\begin{bmatrix} \hat{u}_{LV} \\ \hat{i}_{Lf} \end{bmatrix} = \begin{bmatrix} G_{v1} & G_{v2} & G_{v3} \\ G_{i1} & G_{i2} & G_{i3} \end{bmatrix} \begin{bmatrix} \hat{u}_s \\ \hat{d}_d \\ \hat{u}_{sc} \end{bmatrix} \tag{10}$$

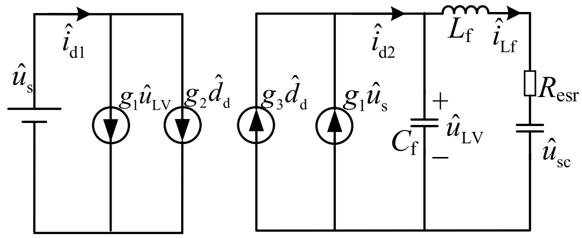

FIGURE 4. Small signal model of DAB module under traditional control strategy.

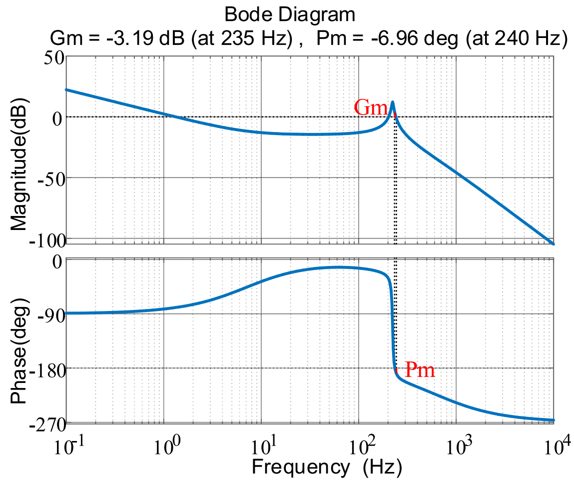

FIGURE 5. Open-loop frequency characteristic curve of DAB converter under traditional control strategy.

Thus, the transfer function of disturbance source $\hat{d}_d$ to state variable $\hat{i}_{LF}$ is expressed as,

$$\left.\frac{\hat{i}_{Lf}(s)}{\hat{d}_d(s)}\right|_{\hat{u}_{sc}(s)=0,\hat{u}_s(s)=0} = G_{i2} = \frac{g_3}{L_f C_f s^2 + C_f R_{esr} s + 1} \tag{11}$$

Therefore, the open-loop transfer function G_1 of DAB converter under single -loop current control can be expressed as,

$$G_1 = G_{ca} G_{i2} H_i \tag{12}$$

where, $G_{ca} = 0.0002 + 0.009/s$ is the transfer function of the PI regular of the current loop. H_i is the equivalent transfer function of the digital delay.

In Fig. 5, the frequency characteristic curve of open-loop transfer function under traditional control strategy is drawn by MATLAB. Among them, Gm is the amplitude margin of the open-loop transfer function of the closed-loop system, and Pm is the phase margin of the open-loop transfer function of the closed-loop system, which are used to measure the relative stability of the closed-loop system. According to the control theory, the stability of the closed-loop control system can be reflected by judging whether the amplitude margin Gm>0dB and the phase margin Pm>0° are satisfied. As shown in Fig. 5, the amplitude margin Gm is −3.19 dB, and the phase margin Pm is −6.96°, which indicates that the DAB control system is unstable under the traditional control strategy.

The frequency of 240Hz in Fig. 5 is actually the cutoff frequency of the open-loop transfer function.

In the above traditional control strategy, there are multiple PI regulators including the current control of MVDC bus, sub-module capacitor voltage balancing control of MMC and current control of DAB. There are many control variables, different regulators affect each other, and PI parameters are difficult to adjust. At the same time, when the DAB converter controls the current of the energy storage port, the system damping is small, which is difficult to realize the rapid charging and discharging of the super capacitor, and it may be also a problem of system instability.

IV. INDEPENDENT CONTROL STRATEGY OF SUB-MODULE CAPACITOR VOLTAGE AND MODELING

When DAB is connected with energy storage units such as super capacitor, the charging or discharging current is difficult to control, so it is necessary to set filter inductance or interface converter at the input port of super capacitor, but this will increase the structural complexity and volume weight of the system. In order to control the charging and discharging current of super capacitor more conveniently, the DAB converter in each branch independently controls each sub-module capacitor voltage without controlling the charging or discharging current, which can simplify the converter structure and reduce the volume and weight of the system. The control strategy proposed in this paper will be further described in detail below.

As shown in Fig. 6, under the control strategy proposed in this paper, MMC adopts double closed-loop control. The inner loop takes the inductance current on the MVDC side as the control objective, and the control objective of the outer loop is decided according to the operating mode. In different modes, the control objective of DAB converter of each branch is always the voltage of sub-module capacitor, which is controlled by N independent voltage regulators. The port on MVDC side has two operating modes: (1) Mode 1 is that a bidirectional power source is connected to the MVDC bus to realize the bidirectional energy flow between the MVDC bus and super capacitor. In Mode 1, the control objective of the outer loop of MMC is the DAB output current, which indicates the total power of MMC-DAB. (2) Mode 2 is to connect the resistive load at the MVDC side, and the super capacitor supplies power to the resistive load. In order to maintain the continuity of the ship's power supply, in Mode 2, the control objective of the MMC outer loop is MVDC bus voltage.

From Fig. 6, $i_{\mathrm{DAB\_ref}}$ and $i_{\mathrm{DAB\_mean}}$ are respectively the reference value and the average of actual value of charging or discharging current of super capacitor. $i_{\mathrm{MV\_ref}}$ and i_{MV} are respectively the reference value and actual value of the current of the MVDC bus. $u_{\mathrm{s\_ref}}$ and $u_{\mathrm{s1}} \sim u_{\mathrm{s}i}$ are the reference value and actual value of the voltage of each sub-module capacitor respectively. $d_{\mathrm{d1}} \sim d_{\mathrm{dN}}$ are the outer phase-shift ratio of the DAB converter of each branch generated by the voltage loop.

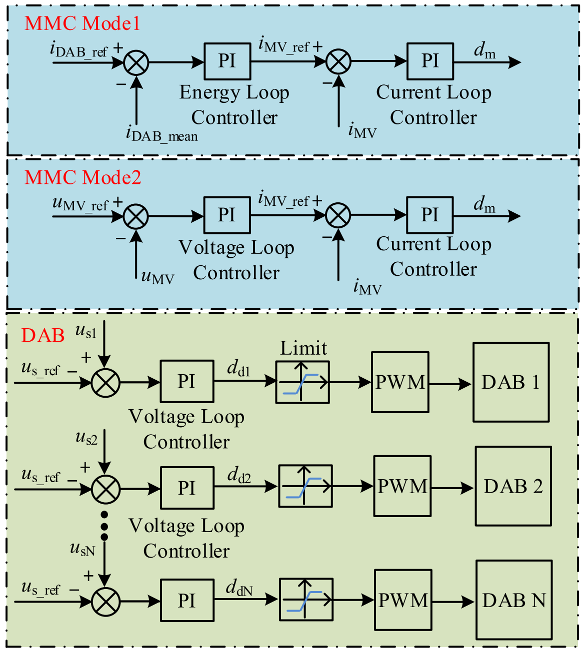

FIGURE 6. Block diagram of independent control strategy of sub-module capacitor voltage for MMC-DAB.

In Mode 1, the control objective of MMC inner loop is the current of the MVDC bus. The actual value i_{MV} of the current of the MVDC bus is subtracted from the reference value $i_{\mathrm{MV\_ref}}$ of the bus current generated by the outer loop controller. Then the sub-module duty ratio d_{m} is generated through the PI controller. The outer loop is the energy loop of the whole system, which is used to regulate the system power and the charging or discharging current of the super capacitor. The difference between the reference output current $i_{\mathrm{DAB\_ref}}$ of each DAB and the average current $i_{\mathrm{DAB\_mean}}$ of all the N DAB is calculated, then the reference current $i_{\mathrm{MV\_ref}}$ of the MVDC bus is generated through the PI regulator. And, the output of the PI regulator is limited according to the actual situation. The control strategy of Mode 1 can be applied to the condition of bidirectional flow of energy.

In Mode 2, because the resistance is connected at the MVDC side, it is necessary to control the resistance voltage on the MVDC side. So, the outer loop of MMC is responsible to regulate the MVDC bus voltage. The actual value of the voltage u_{MV} of the MVDC bus is subtracted from the voltage reference $u_{\mathrm{MV\_ref}}$. The voltage error is sent to the PI regulator to generate the current reference on the MVDC side. The inner control loop of Mode 2 is the same as Mode 1. This control strategy is suitable for the condition that the super capacitor energy storage system on the LVDC side supplies power to resistance on the MVDC side.

Regardless of the operating mode of the MMC, the control objective of the DAB converter of each branch is always the voltage of the sub-module capacitor. The voltage loop regulator adopted by DAB of each branch independently controls the sub-module capacitor voltage. For DAB voltage matching control, the voltage reference value of the sub-module is $u_{\mathrm{s\_ref}} = n_{\mathrm{T}} u_{\mathrm{sc}}$. Since it is a negative feedback

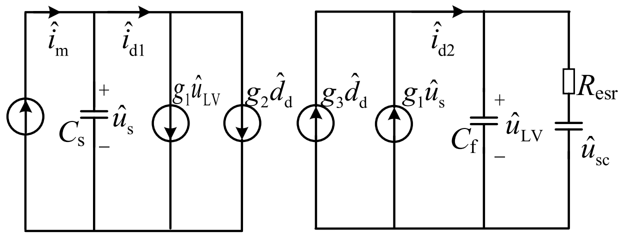

FIGURE 7. The small signal model of DAB converter under the independent control strategy of sub-module capacitor voltage.

system, the actual value u_{si} subtracts the reference value u_{s_ref}. Then, the phase-shift ratio d_{di} of DAB is generated through PI controller and the driving pulse signal is generated through PWM generator.

When the DAB controls the voltage of the sub-module capacitor without controlling the current of the super capacitor energy storage system, the filter inductance can be omitted. The load at the primary side of the DAB converter can be equivalent to a current source. Therefore, its small signal model is shown in Fig. 7.

Since the LVDC bus is connected to the energy storage unit, it can be considered that the voltage on LVDC side is constant. Then the voltage of the sub-module capacitor is selected as the state variable for modeling. And its state equation can be expressed as

$$C_{\mathrm{s}}\frac{d\hat{u}_{\mathrm{s}}}{dt}=\hat{i}_{\mathrm{m}}-\hat{i}_{\mathrm{d1}}=\hat{i}_{\mathrm{m}}-\left(g_1\hat{u}_{\mathrm{LV}}+g_2\hat{d}_{\mathrm{d}}\right) \tag{13}$$

Laplace transformation is implemented on the above state equation, so the transfer function from disturbance source to state variable is written as

$$\begin{aligned} G_{\mathrm{D1}} &= \frac{\hat{u}_{\mathrm{s}}(s)}{\hat{u}_{\mathrm{LV}}} = \frac{-g_1}{sC_{\mathrm{s}}} \\ G_{\mathrm{D2}} &= \frac{\hat{u}_{\mathrm{s}}(s)}{\hat{d}_{\mathrm{d}}} = \frac{-g_2}{sC_{\mathrm{s}}} \\ G_{\mathrm{D3}} &= \frac{\hat{u}_{\mathrm{s}}(s)}{\hat{i}_{\mathrm{m}}} = \frac{1}{sC_{\mathrm{s}}} \end{aligned} \tag{14}$$

where, the transfer function of the outer phase-shift ratio $\hat{d}$d of DAB to the capacitor voltage of sub-module is G_{D2}.

Therefore, the open-loop transfer function G_2 of the proposed closed-loop control system can be obtained as follows.

$$G_2 = G_{\mathrm{cv}}G_{\mathrm{D2}}H_{\mathrm{i}} \tag{15}$$

where $G_{\mathrm{cv}} = 0.0002 + 0.009/s$ is the transfer function of PI regulator of independent voltage loop control, and H_{i} is the equivalent transfer function of the digital delay.

The frequency characteristic curve of open-loop transfer function G_2 is drawn by MATLAB, as shown in Fig. 8. According to the curve, the system stability margin of the independent control strategy of the sub-module voltage is large, whose amplitude margin Gm is infinite, and the phase margin Pm is 72.7°. The above results show that under the proposed control strategy, the phase margin Pm and the amplitude margin Gm of the system satisfy the stability criterion. The frequency of 180Hz in Fig. 8 is the cutoff frequency of the open-loop transfer function under the proposed control strategy, which is related to control structure and control parameters.

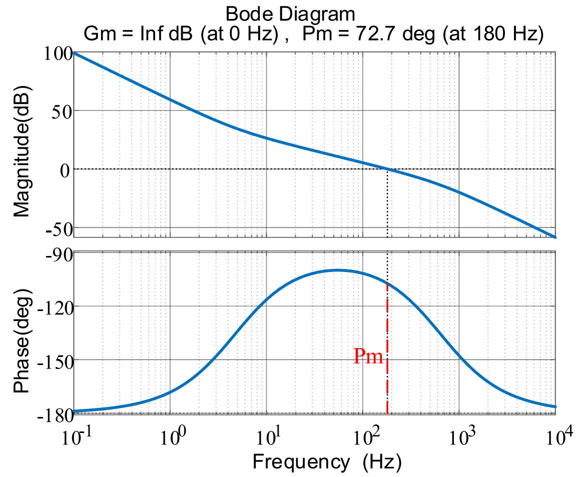

FIGURE 8. Open-loop frequency characteristic curve of DAB converter under the independent control strategy of sub-module capacitor voltage.

TABLE 1. The prototype parameters of super capacitor energy storage system based on MMC-DAB.

Parameter	Value
Rated voltage of the MVDC bus U_{MV}/V	10000
Rated voltage of supercapacitor U_{sc}/V	834~1166
Capacitance value of super capacitor C_{sc}/F	41.67
Inductance on the MVDC side L_{MV}/mH	2.5
Sub-module capacitance C_{s}/mF	1
Transformer ratio of DAB n_{T}	8:5
Transformer leakage inductance L_{s}/mH	0.2
Filter capacitor C_{f}/mF	3
Switching frequency of MMC f_{m}/Hz	4000
Switching frequency of DAB f_{d}/Hz	4000

V. EXPERIMENTAL RESULTS

To verify the above theoretical analysis, a super capacitor energy storage system based on MMC-DAB is designed and manufactured. The parameters and physical drawings of the prototype are shown in Table 1 and Fig. 9 respectively. In Fig. 9, The prototype consists of eight branch cabinets, medium-voltage side circuit cabinet, control cabinet, water-cooled cabinet and two super capacitor energy storage units of slow charging and fast discharging type. The input port of the converter is connected with 10kV DC bus and the output port is the LVDC bus, which is connected with the super capacitor energy storage unit. There is an upper limit for the super capacitor voltage. When the super capacitor charging reaches the upper limit voltage, the controller will automatically set the current reference to zero. The lower limit of the super capacitor voltage is considered in the discharging state. When the super capacitor is discharged to the lower limit voltage, the current reference will also be set to zero automatically.

The experimental schematic diagram of the engineering prototype in this paper is shown in Fig. 10. The main circuit

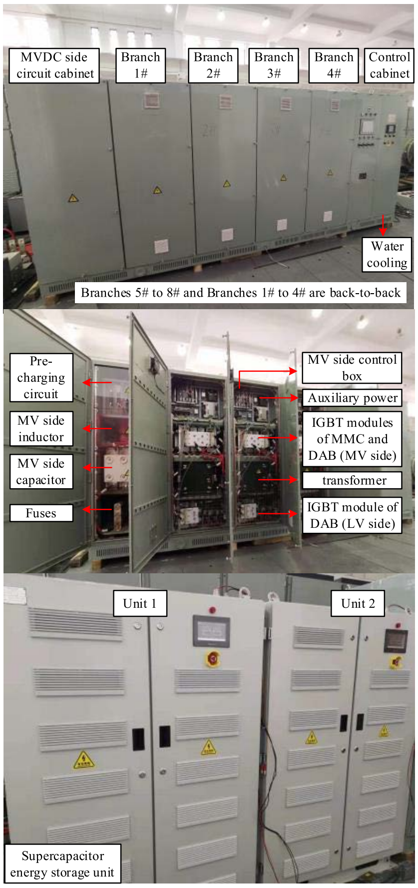

FIGURE 9. Schematic diagram of the prototype of the MW-level supercapacitor energy storage system.

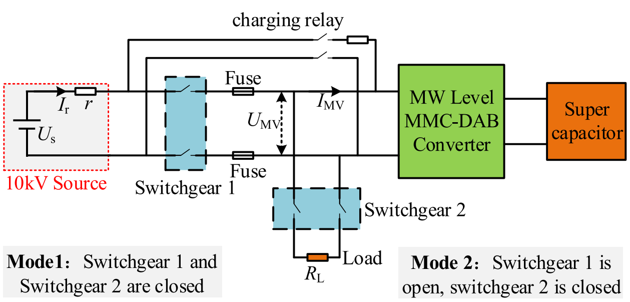

FIGURE 10. Experimental schematic diagram of MW-level supercapacitor energy storage system.

includes the 10kV uncontrolled rectifier DC power source with internal resistance r, switchgear, charging relay and 1MW super capacitor energy storage system. When both switchgear 1 and switchgear 2 are closed, the MMC-DAB system works under Mode 1. At this time, the bidirectional charging and discharging experiment of energy storage system is carried out. When switchgear 1 is open and switchgear 2 is closed, the system works in Mode 2. At this time, a resistive load is connected to on the MVDC bus for super capacitor discharging experiment.

The prototype platform adopts a layered control structure and a high-speed optical fiber ring network communication structure, as shown in Fig. 11. The controller consists of a

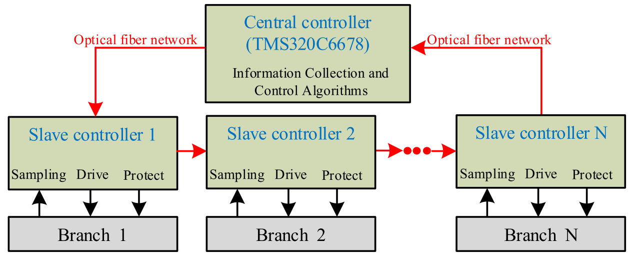

FIGURE 11. Distributed control architecture for loop network communication of converter prototype controller.

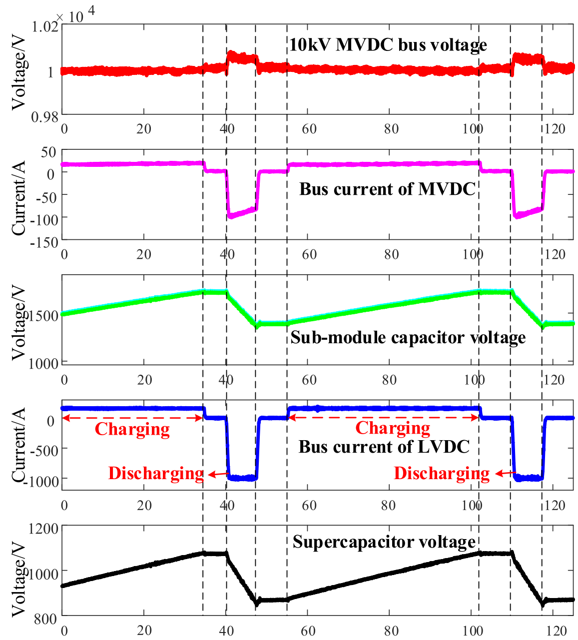

FIGURE 12. Experimental waveforms of charging and discharging for MW-level super capacitor energy storage system in Mode 1.

central controller and N slave controllers, which is conducive to modulization, standardization and redundant protection. The central controller communicates and exchanges information with the slave controller through the optical fiber ring network. The slave controller usually contains a Field Programmable Gate Array (FPGA) as a control chip, which is responsible for sensor data sampling, driving pulse generation and hardware protection. The central controller includes a digital signal processor (DSP) and FPGA as the control chip, which is responsible for the operation of the top-level control algorithm and the collection of the bottom-level data. Finally, the experimental data is uploaded to the upper computer through Ethernet for record and storage.

In Mode 1, a 60 Ω resistive load is connected to the MVDC side and the charging and discharging experimental waveform of 1MW modular super capacitor energy storage system is shown in Fig. 12. In Fig. 12, the experimental waveforms of the voltage and current of the MVDC bus, sub-module capacitor voltage, super capacitor voltage and super capacitor current are given. Under the charging state, the 10kV DC power source supplies power to the super capacitor energy storage unit through the converter. The reference value of

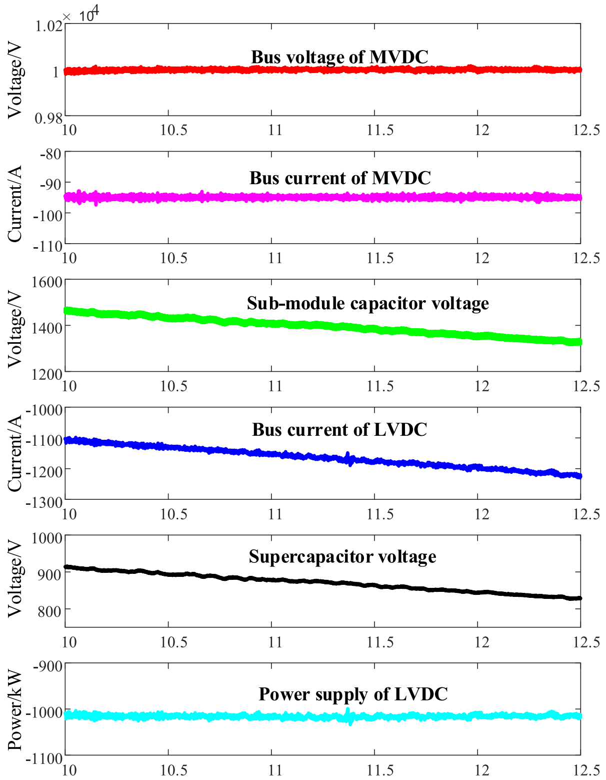

FIGURE 13. Experimental waveform of discharge of MW-level super capacitor energy storage system in Mode 2.

the single branch current command of the DAB module is 20A. At this time, the charging current of the super capacitor is 160A, the charging power reaches 160kW, and the super capacitor voltage rises evenly from 860V to 1080V. Besides, since the voltage at both ends of the DAB is controlled by voltage matching strategy, the sub-module capacitor voltage increases from 1376V to 1728V with the change of the super capacitor voltage value. When the reference value of single branch current command of DAB module is 0A, there is no power flow, the current of the LVDC bus is 0, and the supercapacitor voltage is basically unchanged. Under the discharging state, the reference value of the single branch current command of the DAB module is 125A. At this time, the discharging current of the LVDC bus is 1000A, and the supercapacitor voltage decreases evenly from 1080V to 860V. The sub module capacitor voltage command changes with the supercapacitor voltage value from 1728V to 1376V, and the discharge power of the system reaches 1MW. In Fig. 12, during the switching of charging and discharging current commands, the load at both ends of the MVDC grid fluctuates, and the internal resistance current I_r decreases, which causes the voltage waveform of the MVDC bus to fluctuate. But the voltage fluctuation is 1%, which is within the acceptable range. Therefore, the super capacitor energy storage unit can maintain the short-term support of the power grid energy at the MVDC side, ensuring the reliability and sustainability of the power supply of the MVDC bus, making the energy flow more flexible.

In Mode 2, a 105 Ω resistive load is connected to the MVDC side, and the discharging experimental waveform of the super capacitor is shown in Fig. 13. At this time, the MMC adopts the outer voltage loop on the MVDC side, the super capacitor energy storage system discharges at constant power, and the reference value of the voltage command on the MVDC side is 10kV. At this time, the current of the MVDC bus is 95A, the super capacitor voltage and the current of the LVDC bus decrease evenly, and the discharging power of the super capacitor reaches 1MW.

Experiments results show that the proposed independent control strategy of sub-module capacitor voltage can realize the good charging and discharging performance for super capacitor energy storage system. The actual power and current can follow the reference to charging and discharging of the super capacitor. The ripple coefficient of charging and discharging current of super capacitor is less than 5%, and the current of each branch of energy storage port shows good consistency. The response of the dynamic current command switching is fast, and the changing rate of charging and discharging current is 2000 A/s.

VI. CONCLUSION

A cascaded super capacitor energy storage system based on MMC-DAB for vessel integrated power system is studied in this paper. The super capacitor energy storage unit is connected to LVDC bus, which is conducive to enhance the flexibility and reliability of the energy regulation of shipboard DC grid, and also provides power source for pulse loads on board. The traditional control strategy and the proposed independent control strategy of sub-module capacitor voltage are compared and analyzed. The mathematical models of DAB converters under the two control strategies are established, and the stability characteristics of them are compared. Under the proposed control strategy, the amplitude margin of DAB is infinite and the phase stability margin is 72.7°, while under the traditional control strategy, the system presents an unstable state. Therefore, the system has better stability under the proposed control strategy. Finally, a modular and standardized engineering prototype of 1MW is designed and manufactured, and the experimental results are analyzed to verify the correctness of the theoretical analysis and control strategy design. This paper provides an effective solution for the development of MW-class modular energy storage converter.

REFERENCES

[1] W. Ma, "On comprehensive development of electrization and informationization in naval ships," *J. Nav. Univ. Eng.*, vol. 22, no. 5, pp. 1–4, Oct. 2010.
[2] M. Weiming, "Development of vessel integrated power system," in *Proc. Int. Conf. Electr. Mach. Syst.*, Beijing, China, Aug. 2011, pp. 1–12.
[3] W. Ma, "Development of vessel integrated power system," *Ordnance Knowl.*, vol. 4, no. 3, pp. 31–33, 2011.
[4] L. Fu, L. Liu, G. Wang, F. Ma, Z. Ye, F. Ji, and L. Liu, "The research progress of the medium voltage DC integrated power system in China," *Chin. J. Ship Res.*, vol. 11, no. 1, pp. 72–99, Feb. 2016.
[5] S. Wan and Z. Meng, "Current status and prospects of analysis technologies of shipboard integrated power system," *Chin. J. Ship Res.*, vol. 14, no. 2, pp. 107–117, Apr. 2019.

[6] L. Qu, "Study on key technique of input series combination converters control strategy," Ph.D. dissertation, Shenzhen Graduate School, Harbin Inst. Technol., Shenzhen, China, 2018.

[7] F. An, W. Song, and K. Yang, "Model predictive control and power balance scheme of dual-active-bridge DC–DC converters in power electronic transformer," *Proc. CSEE*, vol. 38, no. 13, pp. 3921–3929, Jul. 2018.

[8] W. Chen, X. Ruan, and H. Yan, "Control strategy for DC/DC multiple modules series-parallel combined systems," *Trans. China Electrotech. Soc.*, vol. 24, no. 7, pp. 93–102, Jul. 2009.

[9] L. Qu, D. Zhang, and Z. Bao, "Output current-differential control scheme for input-series–output-parallel-Connected modular DC–DC converters," *IEEE Trans. Power Electron.*, vol. 32, no. 7, pp. 5699–5711, Jul. 2017.

[10] H. Zhang, W. Shao, X. Wei, and N. Li, "Study on fault tolerant control strategy for sub-modules of modular multilevel converter," in *Proc. Asia Energy Electr. Eng. Symp. (AEEES)*, Chengdu, China, May 2020, pp. 416–420.

[11] W. Wu, S. Xie, Z. Zhang, and J. Xu, "Analysis and design of control strategy for MMC-BDC based ultra-capacitors energy storage systems," *IEEE Trans. Power Electron.*, vol. 34, no. 27, pp. 4568–4575, Sep. 2014.

[12] K. Bi, L. Sun, Q. An, J. Duan, and Y. Gao, "Distributed energy balancing control strategy for energy storage system based on modular multilevel DC–DC converter," *Trans. China Electrotech. Soc.*, vol. 33, no. 16, pp. 3811–3821, Aug. 2018.

[13] N. Li, L. Zhang, S. Ma, and F. Gao, "Control strategy for battery energy storage system based on modular multilevel converters," *Autom. Electr. Power Syst.*, vol. 41, no. 9, pp. 144–150, May 2017.

[14] K. Bi, Q. An, D. Sun, J. Duan, and L. Sun, "Modular multilevel energy storage system open circuit diagnostic method based on sub-module operation analysis," *Trans. China Electrotech. Soc.*, vol. 33, no. 6, pp. 1219–1226, Mar. 2018.

[15] F. Krismer and J. W. Kolar, "Efficiency-optimized high-current dual active bridge converter for automotive applications," *IEEE Trans. Ind. Electron.*, vol. 59, no. 7, pp. 2745–2760, Jul. 2012.

[16] F. Xue, R. Yu, and A. Q. Huang, "A 98.3% efficient GaN isolated bidirectional DC–DC converter for DC microgrid energy storage system applications," *IEEE Trans. Ind. Electron.*, vol. 64, no. 11, pp. 9094–9103, Nov. 2017.

[17] Y. W. Cho, W. J. Cha, J. M. Kwon, and B. H. Kwon, "High-efficiency bidirectional DAB inverter using a novel hybrid modulation for stand-alone power generating system with low input voltage," *IEEE Trans. Power Electron.*, vol. 31, no. 6, pp. 4138–4147, Jun. 2016.

[18] J. Li, B. Zhao, Q. Song, Y. Huang, Q. Sun, Y. Wang, and W. Liu, "DC solid state transformer based on multilevel DC link for medium-voltage DC distribution application," *Proc. CSEE*, vol. 36, no. 14, pp. 3717–3726, Jul. 2016.

[19] Y. Wang, Q. Song, Q. Sun, B. Zhao, J. Li, and W. Liu, "Multilevel MVDC link strategy of high-frequency-link DC transformer based on switched capacitor for MVDC power distribution," *IEEE Trans. Ind. Electron.*, vol. 64, no. 4, pp. 2829–2835, Apr. 2017.

[20] J. Liu, Z. Zhu, F. Xiao, P. Chen, and Q. Ren, "A modular three-port DC–DC converter for vessel integrated power system," *Trans. China Electrotech. Soc.*, vol. 35, no. 19, pp. 4085–4096, Oct. 2020.

[21] Y. Guan, Y. Xie, Y. Wang, Y. Liang, and X. Wang, "An active damping strategy for input impedance of bidirectional dual active bridge DC–DC converter: Modeling, shaping, design, and experiment," *IEEE Trans. Ind. Electron.*, vol. 68, no. 2, pp. 1263–1274, Feb. 2021.

ZHICHAO ZHU was born in Fujiang, China, in 1994. He received the B.S. degree from the Naval University of Engineering, Wuhan, China, in 2017, where he is currently pursuing the Ph.D. degree.

His current research interests include modular multilevel converter and large-capacity energy storage converter.

FEI XIAO was born in Hubei, China, in 1977. He received the B.S. and M.S. degrees in electrical engineering from the Naval University of Engineering, Wuhan, China, in 1999 and 2001, respectively, and the Ph.D. degree in electrical engineering from Zhejiang University, in 2012. From 2003 to 2009, he was a Lecturer with the Naval University of Engineering. He was promoted to an Associate Professor, in 2009, and to a Full Professor, in 2012. He is also the Committee Member of the Department of Energy and Transportation, China Ministry of Science and Technology. His current research interests include renewable energy generation, modeling and control of power electronics systems, and high-voltage large-capacity power electronics equipment.

ZHAOJIE HUANG was born in Hubei, China, in 1995. He received the B.S. degree from the School of Transportation, Wuhan University of Technology, Wuhan, China, in 2017, and the master's degree from the College of Shipbuilding Engineering, Harbin Engineering University, Wuhan, in 2020. He is currently pursuing the Ph.D. degree with the Department of Electrical Engineering, Naval University of Engineering, Wuhan. His current research interests include power conversion systems and multiport bidirectional DC–DC converter.

JILONG LIU was born in Hebei, China, in 1988. He received the B.S. and Ph.D. degrees from the School of Electrical Engineering, Xi'an Jiaotong University, Xi'an, China, in 2010 and 2015, respectively.

From 2015 to 2017, he was a Lecturer with the National Key Laboratory of Science and Technology on Vessel Integrated Power System, Naval University of Engineering, Wuhan, China. He was promoted to an Associate Professor, in 2017. His current research interests include modular multilevel converter and AC motor control.

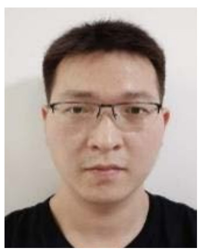

PENG CHEN was born in Jiangsu, China. He received the B.S. degree in electrical engineering from Southeast University, Nanjing, China, in 2016, where he is currently pursuing the Ph.D. degree in electrical engineering.

He has been working as a joint Training Student with the National Key Laboratory for Vessel Integrated Power System Technology, Wuhan, China, since 2017. His research interests include modular multilevel DC–DC converter and control strategies for multiport converter.

QIANG REN was born in Sichuan, China, in 1989. He received the B.S. degree in electronic information engineering from the Ocean University of China, Shandong, China, in 2008, and the Ph.D. degree in electrical engineering from the Naval University of Engineering, Hubei, China.

He is currently a Lecturer with the Naval University of Engineering. His research interests include power electronics and power transmission.